Heliyon 9 (2023) e16999

Contents lists available at ScienceDirect

Heliyon

journal homepage: www.cell.com/heliyon

LINC00638 promotes the progression of non-small cell lung cancer by regulating the miR-541-3p/IRS1/PI3K/Akt axis

Juan Zhang [a,b], Yanhua Mou [a,b], Hui Li [a,b], Hui Shen [a,b], Jun Song [a,b], Qingfeng Li [a,b,*]

[a] Department of Oncology, Xiangyang Central Hospital, Affiliated Hospital of Hubei University of Arts and Science, Xiangyang 441021, Hubei, China
[b] Institute of Oncology, Xiangyang Central Hospital, Affiliated Hospital of Hubei University of Arts and Science Hubei University of Arts and Science, Xiangyang 441021, Hubei, China

ARTICLE INFO

Keywords:
Non-small cell lung cancer
Progression
LINC00638
miR-541-3p
Insulin receptor substrate 1

ABSTRACT

Background: Preceding works reveal the function of long non-coding RNAs (abbreviated to lncRNAs) during non-small cell lung cancer (NSCLC) evolvement. We explored the profile and biological functions of the lncRNA LINC00638 in NSCLC.

Methods: Reverse transcription-quantitative PCR examined LINC00638 level in NSCLC and corresponding non-tumor tissues, human normal lung epithelial cells BEAS-2B, and NSCLC cells (NCI–H460, HCC-827, A549, H1299, H1975, H460). The gain- and loss-of-function assay of LINC00638 ascertained its function in modulating the proliferation, apoptosis, and invasion of NSCLC cells (HCC-827 and H460). Bioinformatics analysis investigated the underlying mechanisms. Dual luciferase reporter gene and RNA immunoprecipitation (RIP) checked the interactions between LINC00638 and microRNA (miR)-541-3p, miR-541-3p and insulin receptor substrate 1 (IRS1).

Results: LINC00638 was upregulated in NSCLC tissues by contrast to the profiles found in the corresponding non-tumor normal tissues, as well as in NSCLC cells vis-à-vis BEAS-2B cells. LINC00638 upregulation pertained to the poorer survival rates of NSCLC patients. Overexpressing LINC00638 augmented NSCLC cells' proliferation, growth, migration, and invasion but inhibited their apoptosis, while down-regulating LINC00638 led to the opposite. miR-541-3p might be an underlying target of LINC00638, which targeted IRS1, inhibited NSCLC progression, and reversed the carcinogenic effects of LINC00638. Mechanistically, LINC00638/miR-541-3p regulated the IRS1/phosphoinositide 3-kinase (PI3K)/Akt signaling pathway. Repressing IRS1/2 using its inhibitor NT157 repressed LINC00638-mediated oncogenic effects.

Conclusion: LINC00638 may function as an oncogene in NSCLC by modulating the miR-541-3p/IRS1/PI3K/Akt axis.

1. Introduction

As one of the most prevailing malignancies across the world, lung cancer is the primary contributor to cancer-correlated mortality

* Corresponding author. Department of Oncology & Institute of Oncology, Xiangyang Central Hospital, Affiliated Hospital of Hubei University of Arts and Science, No. 136 Jingzhou Street, Xiangyang 441021, Hubei, China.
E-mail address: liqingfengdoc@163.com (Q. Li).

https://doi.org/10.1016/j.heliyon.2023.e16999
Received 28 December 2022; Received in revised form 31 May 2023; Accepted 2 June 2023
Available online 15 June 2023

in men and women [1]. Non-small cell lung cancer (NSCLC) makes up approximately 85% of all lung cancer cases among the multiple pathological types of lung cancer, with a 5-year survival rate below 20% in that >60% of patients diagnosed with NSCLC enter the advanced stage [2,3]. Despite the efforts of previous studies to identify more effective targeted therapies for treating NSCLC, primary and acquired resistance limit their clinical benefits [4–6]. As a result, exploring the pathogenesis and progression of NSCLC is important for its early diagnosis and targeted therapy.

Long non-coding RNAs (lncRNAs) are endogenous ncRNAs consisting of >200 nucleotides (nt) [7]. LncRNAs are emerging as important players in various biological processes, including gene regulation, chromatin remodeling, and epigenetic modification [8,9]. Noteworthily, lncRNAs take part in the progression of cancers as oncogenes and tumor suppressors [10]. For instance, lncRNA MAPKAPK5-AS1, upregulated in lung cancer tissues, bolsters lung cancer proliferative and migratory capacities whereas reduces apoptotic level via upregulating CAB39 [11]. Similarly, overexpression of the lncRNA ZXF1 enhances lung adenocarcinoma progression by promoting tumor cell invasion and metastasis [12]. As a new member in the lncRNA family, LINC00638 is situated on chromosome 14: 104,821,201–104,823,718 forward strand with 2,518 nt in length. LINC00638 is differentially expressed in lumbar disc degeneration versus normal intervertebral discs [13]. In liver cancer, upregulated LINC00638 is associated with tumor mutation burden (TMB) and immune infiltration and potentially regulates the miR-4732-3p/ULBP1 axis [14]. Nevertheless, the profile and mechanism of LINC00638 in the context of NSCLC are worth exploring.

MicroRNAs (abbreviated to miRNAs or miRs) are endogenous ncRNAs with 20–24 nt in length. miRNAs bind to the 3′-untranslated region (3′-UTR) of their targeted genes to modulate the profiles of genes, hence affecting cellular growth, proliferation, apoptosis, differentiation, and other biological processes [15,16]. Notably, miRNAs show abnormal expressions in various tumors and are closely linked to tumorigenesis tumor development [17]. Additionally, miRNAs also function significantly in NSCLC. For instance, miR-140-3p has potential as a therapeutic target to enhance the sensitivity of LUAD to chemotherapy by targeting the ADAM10/Notch pathway [18]. miR-541-3p partakes in tumor development. It is negatively modulated by the lncRNA LOXL1-AS1 and targets cyclin D1, thereby inhibiting tumor cell proliferation and cycle progression [19].

Our research detected the LINC00638 level in NSCLC to explore LINC00638 expression alteration in NSCLC tissues and its association with the survival of NSCLC patients. Functional studies were performed to confirm the impact of LINC00638 on NSCLC cell proliferation, apoptosis, and invasion. Bioinformatics analysis was conducted to explore the downstream of LINC00638 in NSCLC progression. All over, this research probed the molecular mechanism of the LINC00638/miR-541-3p/IRS1 axis in NSCLC development in the hope of providing a potential diagnosis and therapy target for lung cancer.

2. Materials and methods

2.1. Collection of patient samples

42 paired NSCLC tissue and adjacent non-tumor specimens were obtained from NSCLC patients who were hospitalized in Xiangyang Central Hospital. These patients had never undergone radiotherapy or chemotherapy prior to surgery. They were diagnosed with NSCLC by two experienced pathologists. With their basic clinical information harvested, the patients were followed up through phone calls. Our study was given the imprimatur by the ethics committee of Xiangyang Central Hospital (Approval No. XYCH-2019-146). All patients agreed to take part in our research with informed consent.

2.2. Culture of cells

American Type Culture Collection supplied the cells we need: normal human bronchial epithelial cells BEAS-2B and NSCLC cells (HCC-827, A549, NCI–H460, H1975, H1299, H460). The cells were grown in DMEM-F12 (Sigma-Aldrich; Merck KGaA) incorporating 10% fetal bovine serum (FBS; Gibco; Thermo Fisher Scientific, Inc.) under the conditions of 5% CO_2 and 37 °C in an incubator. We exchanged the culture medium every 1 or 2 days. Well-grown cells were employed for the following experiments. Trypsin (0.25%; Beyotime Institute of Biotechnology) was utilized for the trypsinization of the cells. The IRS1/2 inhibitor NT157 (1 μM, TOKYO CHEMICAL INDUSTRY CO., LTD., Japan) was used for inhibiting IRS1/2.

2.3. Transfection of cells

Shanghai GenePharma Co., Ltd. designed small interference RNA (siRNA) specifically targeting LINC00638 (si-LINC00638), LINC00638 overexpression plasmids, and their negative controls (si-NC and vector). Guangzhou RiboBio Co., Ltd. provided miR-541-3p mimics, miR-541-3p inhibitors, and miRNA negative controls. HCC-827 and H460 were transfected along with the aforementioned overexpressed or downregulated vectors through Lipofectamine® 3000 (Thermo Fisher Scientific, Inc.) in a line with the supplier's recommendations. Followed by a 24-h incubation (5% CO_2, 37 °C), the cells was cultured with a fresh complete medium substituting the culture medium. RT-qPCR evaluated the LINC00638 level for ascertaining the efficiency of the transfection.

2.4. Detection of cell proliferation

HCC-827 and H460 cells, inoculated on 96-well plates (density: 5×10^3 cells per well), were cultivated for 12, 24, 48, and 72 h preceding the removal of the medium. Next, CCK-8 solution (Beyotime Institute of Biotechnology) was given to the cells for incubation in a standard incubator (5% CO_2, 37 °C). The microplate reader (Multiskan GO; Thermo Fisher Scientific, Inc.) gauged the absorbance

value (450 nm). Six multiple wells were set for each test, and the experiment was implemented in triplicate.

2.5. Cell apoptosis examination

The Annexin V-Alexa Fluor 488/PI kit was used for apoptosis detection (SouthernBiotech). Subsequent to trysinization, the NSCLC cells were centrifuged for 5 min (178g at room temperature (RT)), washed by pre-cold PBS, and then stained by AnnexinV-PE and 7-AAD (TransGen) solution at RT (15 min) in the darkness. At last, flow cytometry evaluated the proportion of stained cells via Flow Cytometer (BD Biosciences).

2.6. Transwell assay

After being trypsinized, the cells were harvested through centrifugation (178g, 5 min; RT) and resuspended in DMEM-F12 free of serum. The concentration of cells was adjusted to 1×10^5 cells/ml. Transwell chambers (8 μm, Corning Inc.) were precoated by BD Matrigel™. The cells were inoculated into the upper Transwell chamber. Next, the lower compartment was added with 500 μl complete DMEM-F12 containing 20% FBS. The plates were put in an incubator for 24 h with 5% CO_2 (37 °C). Subsequently, a cotton swab was utilized to remove the cell that failed invading through the membrane. At the same time, the cells that succeeded in invasion and adhered to the lower compartment were immobilized in 4% paraformaldehyde (15 min, RT) and dyed using 1% crystal violet solution (Beyotime) (15 min, RT). For testing cell migration, Matrigel was not adopted to precoat the chambers. The remaining steps were the same as described above. A microscope (ZEISS Axioscope 5, 200 ×) was used for observing the cells. The invaded or migrated cells were counted using Image J.

2.7. Colony formation assay

After being trypsinized, the NSCLC cells were harvested through centrifugation (178g, 5 min; RT) and resuspended in DMEM-F12.500 NSCLC cells were seeded onto 60-mm dishes. During the next 2-week culture (5% CO_2, 37 °C), the medium was changed every 3 days. As the culture was terminated, methanol (Sigma-Aldrich, St. Louis, MO, USA) was used for cell fixation, followed by crystal violet (Sigma-Aldrich) staining (15 min, RT). A microscope (ZEISS Axioscope) was used for observing colonies and formatted colonies were counted.

2.8. RT-qPCR

LINC00638 and miR-541-3p levels were gauged through fluorescence RT-qPCR. TRIzol® (Invitrogen; Thermo Fisher Scientific, Inc.) was used for isolating total RNA from the cells and tissues. The collected clinical samples were immediately frozen in liquid nitrogen and stored at −80 °C. For total RNA extraction, the specimens were put in a mortar and ground to powder. 100 mg powder was taken and put in an EP tube added with 1 ml TRIzol solution. Total RNA was extracted using the chloroform-isopropanol-ethanol method. After RNA concentration and purity determination, 2 μg total RNA sample was used to prepare 20 RT reactions and reverse-transcribed into cDNAs by harnessing the RevertAid First Strand cDNA Synthesis Kit (Thermo Fisher Scientific, Inc.). Later, 2 μl of cDNA samples were employed to prepare a 50 μl-qPCR system, which included SYBR Green qPCR Master Mix (MedChemExpress). Finally, qPCR was implemented through the CFX96 Real-Time PCR Detection System (Bio-Rad Laboratories, Inc.). The conditions for the reaction included 2 min at 94 °C and 35 cycles in total (30 s at 94 °C and 45 s at 55 °C). The endogenous control of LINC00638 was GAPDH, while U6 served as the endogenous control of miR-541-3p. The $2^{-\Delta\Delta Ct}$ method was harnessed for calculating the relative level of detected genes. Table 1 details the primers we adopted for the experiment.

Table 1
The sequences of the used PCR primers.

Gene name	Forward primers	Reverse primers
LINC00638	5′-TTCGACCCGTAACAGCTTCT-3′	5′-AGGTCCGTGGAAAACTAGGG-3′
miR-541-3p	5′-AACAAGTGGTGGGCACAGAATC-3′	5′-CAGTGCAGGGTCCGAGGT-3′
miR-6882-3p	5′-AACAAGTGCTGCCTCTCCTCTT-3′	5′-AACAAGTGCTGCCTCTCCTCTT-3′
miR-3138	5′-AAGAGCGTTGTGGACAGTGAG-3′	5′-CAGTGCAGGGTCCGAGGT-3′
miR-7155-5p	5′-AACAATTCTGGGGTCTTGGGC-3′	5′-CAGTGCAGGGTCCGAGGT-3′
miR-645	5′-AACACGTGTCTAGGCTGGTACTG-3′	5′-CAGTGCAGGGTCCGAGGT-3′
miR-6825-5p	5′-AACAAGTGGGGAGGTGTGGAG-3′	5′-CAGTGCAGGGTCCGAGGT-3′
miR-1976	5′-AACAATCCTCCTGCCCTCCTTG-3′	5′-CAGTGCAGGGTCCGAGGT-3′
miR-3150a-3p	5′-AACAAGCAACCTCGACGATCTC-3′	5′-CAGTGCAGGGTCCGAGGT-3′
miR-4520-3p	5′-AACAAGTTGGACAGAAAACACGC-3′	5′-CAGTGCAGGGTCCGAGGT-3′
miR-654-5p	5′-AACAAGTGGTAAGCTGCAGAACA-3′	5′-CAGTGCAGGGTCCGAGGT-3′
GAPDH	5′-GCACCGTCAAGCTGAGAAC-3′	5′-TGGTGAAGACGCCAGTGGA-3′
U6	5′-CTCGCTTCGGCAGCACA-3′	5′-ACGCTTCACGAATTTGCGTGTC-3′

2.9. Western blot

After cell treatment, we removed the culture medium. RIPA lysis buffer (Roche Diagnostics) isolated the total protein. Next, 5 μg total protein was placed on 12% SDS-polyacrylamide gel (100V, 2 h) and transferred to polyvinylidene fluoride membranes. 5% skimmed milk was taken for membrane blocking at RT, and 1% TBS incorporating Tween-20 (TBST) flushed the membranes 3 times (10 min each). The membranes were incubated with primary antibodies including anti-IRS1 (Abcam; cat. no. ab40777; 1:1,000), anti-phosphorylated (p)-PI3K (Abcam; cat. no. ab182651; 1:1,000), anti-PI3K (Abcam; cat. no. ab151549; 1:1,000), anti-p-Akt (Abcam; cat. no. ab38449; 1:1,000), anti-Akt (Abcam; cat. no. ab8805; 1:1,000), anti-cyclin D1 (Abcam; cat. no. ab16663; 1:1,000), anti-cyclin E1 (Abcam; cat. no. ab33911; 1:1,000), anti-cyclin-dependent kinase (CDK)2 (Abcam; cat. no. ab32147; 1:1,000), anti-CDK4 (Abcam; cat. no. ab108357; 1:1,000), anti-p21 (Abcam; cat. no. ab109520; 1:1,000), anti-E-cadherin (Abcam; cat. no. ab1416; 1:1,000), anti-Vimentin (Abcam; cat. no. ab92547; 1:1,000), anti-N-cadherin (Abcam; cat. no. ab76011; 1:1,000), anti-GAPDH (Abcam; cat. no. ab8245; 1:2,000) and anti-p27 (Abcam; cat. no. ab32034; 1:1,000). After overnight incubation, TBST rinsed the membranes. The goat anti-rabbit secondary antibody labeled with horseradish peroxidase (Abcam; cat.no. ab97051 1:3,000) was utilized for further incubation (RT) for 1 h. Next, TBST flushed them 3 times (10 min for each). At last, the Pierce ECL Western Blotting Substrate kit (Thermo Fisher Scientific, Inc.) was used for protein bands color development. Image J (1.8.0, National Institutes of Health) measured each protein band's gray value. GAPDH was used as the internal control. The uncropped Western blot images were included in the supplementary file (Supplementary Figs. 1–6).

2.10. Bioinformatic analysis

Gene Expression Profiling Interactive Analysis (GEPIA) (http://gepia.cancer-pku.cn/), an online database, analyzed the level of LINC00638 in multiple tumors, as well as the associations between LINC00638 and proteins pertaining to the PI3K-Akt signaling pathway (IRS1 and Akt1). Kaplan-Meier (KM) plotter (http://kmplot.com/analysis/) examined the prognosis of NSCLC patients exhibiting different LINC00638 levels. The binding associations between LINC00638 and miR-541-3p, miR-541-3p, and IRS1 were respectively predicted through the bioinformatics databases LncBase v.2 (http://carolina.imis.athena-innovation.gr/diana_tools/web/index.php) and starBase (http://starbase.sysu.edu.cn/). The microT, mipmap, and Targetscan databases forecast the downstream targets of miR-541-3p. The sharing targets were analyzed via Venny's diagram. Gene function enrichment analysis was performed via DAVID.

2.11. Dual luciferase activity assay

Luciferase reporter gene assay was performed using the Dual-Luciferase® Reporter (DLR™) Assay System (Promega Corporation). Wild-type (WT) and mutant (MT) target sequences were integrated into the pGL3 vector (Promega Corporation) for the construction of reporter vectors including pGL3-LINC00638-wild type (LINC00638-WT), pGL3-LINC00638-mutant (LINC00638-MT), pGL3-IRS1-wild type (IRS1-WT) and pGL3-IRS1-mutant (IRS1-MT). HCC-827 cells were transfected together with LINC00638-WT, LINC00638-MT, IRS1-WT, or IRS1-MT alongside miR-541-3p mimics or miR-NC. Subsequent to the 48-h transfection, we tested the luciferase levels in keeping with the supplier's stipulation and the instrument's operational instructions (Promega Corporation). All tests were implemented in triplicate and were duplicated three times.

2.12. RNA immunoprecipitation (RIP)

RIP analysis was done through the Magna RIP™ RNA-Binding Protein Immunoprecipitation Kit (EMD Millipore), as instructed by the supplier. After reaching 80% confluence, HCC-827 cells were harvested and lysed employing RIPA lysis buffer (Beyotime, cat.no P0013K). Then, the anti-IgG or anti-Ago2 antibodies (conjugated with magnetic beads) were employed for incubating the lysates. Subsequently, proteinase K was added to incubate the lysis for removing the protein. Finally, TRIzol (Invitrogen; Thermo Fisher Scientific, Inc.) was used for extracting the immunoprecipitated RNA. RT-qPCR (as mentioned in the section of RT-qPCR) evaluated LINC00638 level.

2.13. Xenograft tumor in nude mice

The animal center of Wuhan University provided 24 BALB/nude mice (20–22g, 6 weeks old). HCC-827 cells transfected together with LINC00638 overexpression plasmids or the negative control (vector) were harvested, and the cell suspension was made (2×10^7 ml^{-1}). Later, 0.1 ml of the cell suspension was transfused into each nude mouse through the left forelimb. During the next four-week incubation in vivo, the tumor volume was calculated. Finally, phenobarbital sodium (100 mg/kg) was intraperitoneally injected to kill the animals, with their tumors weighed. The Ethics Board of Xiangyang Central Hospital authorized the animal-related study. All these animal procedures abided by the Guidelines for the Care and Use of Experimental Animals issued by the National Institutes of Health.

2.14. Immunohistochemistry

The tumors were immobilized in paraformaldehyde, embedded in paraffin, sectioned (4 μm), deparaffinized, and rehydrated in xylene and graded ethanol (10 min). Citrate buffer (10 mM, pH 6.0) was used for antigen retrieval through heating (100 °C) for 25 min.

10% goat serum was used for sealing the sections. Subsequently, the sections were incubated overnight along with anti-IRS1 (Abcam; cat. no. ab40777; 1:200), anti-p-Akt (Abcam; cat. no. ab38449; 1:200), anti-E-cadherin (Abcam; cat. no. ab1416; 1:100), and anti-Vimentin (Abcam; cat. no. ab92547, 1:150) (4 °C). PBS rinsed them twice. Corresponding secondary antibodies were given for further incubation.

2.15. Analysis of statistics

Through the software called SPSS 13.0 (SPSS, Inc.), we analyzed all our statistics. The statistics were quantified as mean ± standard deviation. These tests were duplicated at least 3 times. One-way analysis of variance, combined with the LSD test, contrasted the data of over two groups. Student's t-test contrasted two groups. The χ^2 test examined the affinity between the LINC00638 profile and the clinical indicators of NSCLC patients. Pearson correlation analysis checked the affinity between LINC00638 and miR-541-3p levels in NSCLC tissues. If $P < 0.05$, statistical significance could be confirmed.

3. Results

3.1. LINC0638 was overexpressed in NSCLC tissues and cells

RT-qPCR revealed that the LINC00638 level was remarkably increased in NSCLC tissues vis-à-vis that of the adjacent normal tissues ($P < 0.05$; Fig. 1A). Higher level of LINC00638 predicted poorer overall survival of NSCLC patients (Fig. 1B). Importantly, in the majority of cancer tissues, which included two types of NSCLC tissues (lung adenocarcinoma, lung squamous cell carcinoma), LINC00638 level was upregulated versus that of normal tissues [data from GEPIA (http://gepia.cancer-pku.cn/); Fig. 1C]. Furthermore, the prognosis of patients with NSCLC exhibiting different levels of LINC00638 expression was analyzed by χ^2 test and KM plotter (https://www.jianshu.com/p/49ceeae7fd95). The results revealed that high levels of LINC00638 expression had a relation to further advanced stages of tumor, larger tumor size and propensity for lymphatic metastasis and also indicated the poorer overall survival and first progression of NSCLC patients ($P < 0.05$; Fig. 1D and E, and Table 2). In addition, RT-qPCR gauged LINC00638 expression in NSCLC cells. As evidenced, LINC00638 expression in NSCLC cells (NCI–H460, HCC-827, A549, H1299, H1975, H460) significantly increased by contrast to that in BEAS-2B cells ($P < 0.05$; Fig. 1F). Our findings demonstrated that LINC00638 might serve as an oncogene in NSCLC.

3.2. The impact of LINC00638 NSCLC cell proliferation, apoptosis, invasion, and cell cycle progression

LINC00638 overexpressed and downregulated cell lines were constructed using HCC-827 and H460 (two cell lines related to NSCLC), respectively ($P < 0.05$; Fig. 2A and B). Through CCK-8 and colony formation assays, we discovered that the proliferation and colony formation ability of NSCLC cells were strengthened after the overexpression of LINC00638, and they were inhibited after

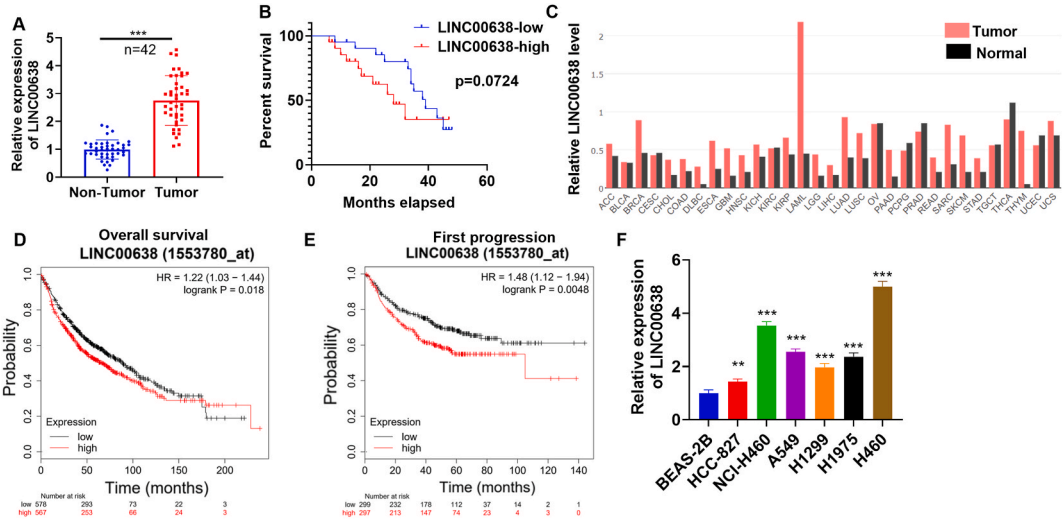

Fig. 1. LINC00638 expression in NSCLC tissues and cells. A: The LINC00638 level in NSCLC tissues and adjacent normal tissues determined through RT-PCR. ***$P < 0.001$. B: The K-M plotter was used for analyzing the association of LINC00638 level and NSCLC patients. C: LINC00638 expression in cancer tissues and normal tissues (data from GEPIA (http://gepia.cancer-pku.cn/)). D and E: The relationship between the LINC00638 level and NSCLC overall survival (D) and first progression (E) analyzed via KM plotter (https://www.jianshu.com/p/49ceeae7fd95). F. The LINC00638 level in BEAS-2B and NSCLC cells (HCC-827, NCI–H460, A549, H1299, H1975, H460) checked by RT-PCR. **$P < 0.01$, ***$P < 0.001$ (vs. BEAS-2B).

Table 2
Correlation between clinicopathological features and LINC00638 expression.

Characteristics	Patients	Expression of LINC00638		P-value
		Low-LINC00638	High-LINC00638	
Total	42	21	21	
Age (years)				0.7683
< 55	20	10	10	
≥55	22	10	12	
Gender				0.334
Male	27	15	12	
Female	15	6	9	
Smoking				0.4945
Yes	30	14	16	
No	12	7	5	
Pathological types				0.9396
Adenocarcinoma	21	11	10	
Squamous carcinoma	13	6	7	
Other	8	4	4	
TNM stage				0.0134*
I-II	20	14	6	
III-IV	22	7	15	
Tumor size				0.0299*
≥5 cm	23	8	15	
< 5 cm	19	13	6	
Lymphatic metastasis				0.0495*
Yes	14	4	10	
No	28	17	11	
Distant metastasis				0.1156
Yes	8	2	6	
No	34	19	15	

Note: * represents $P < 0.05$.

LINC00638 was knocked down ($P < 0.05$; Fig. 2C–E). HCC-827 cell apoptosis was decreased after overexpression of LINC00638, while the apoptosis of H460 cells was enhanced after knocking down LINC00638 ($P < 0.05$; Fig. 2F). The profiles of proteins in HCC-827 and H460 cells were evaluated by Western blot. It was observed that LINC00638 upregulation enhanced cyclin D1, cyclin E1, CDK2, and CDK4 levels and inhibited p21 and p27 levels, while LINC00638 downregulation lowered cyclin D1, cyclin E1, CDK2, and CDK4 levels and boosted p21 and p27 levels (Fig. 2G). Furthermore, the gain- and loss-of-function test of LINC00638 unveiled that LINC00638 enhanced NSCLC cell migration and invasion ($P < 0.05$; Fig. 2H and I). As evidenced by Western blot, LINC00638 upregulation enhanced N-cadherin and Vimentin but repressed the E-cadherin level. Oppositely, LINC00638 knockdown enhanced the E-cadherin level and reduced N-cadherin and Vimentin profiles ($P < 0.05$; Fig. 2J). All these outcomes reflected that LINC00638 partook in NSCLC progression by promoting the proliferation, invasion, migration, and EMT of tumor cells and repressing their apoptosis.

3.3. LINC00638 targeted and inhibited miR-541-3p

The downstream targets of LINC00638 were predicted via LncBase v.2 (http://carolina.imis.athena-innovation.gr/diana_tools/web/index.php). Ten candidate miRNAs were found and detected in LINC00638-overexpressing HCC-827 cells. The statistics verified that miR-541-3p was the most significantly downregulated miRNA (Fig. 3A). Fig. 3B displays the binding sites of miR-541-3p and LINC00638. Furthermore, downregulating LIN00638 markedly enhanced the miR-541-3p level ($P < 0.05$; Fig. 3C). Subsequently, RT-qPCR gauged miR-541-3p profile in NSCLC tissues. As a result, the miR-541-3p level in NSCLC tissues was notably lower compared with that in adjacent normal tissues ($P < 0.05$; Fig. 3D). Moreover, we uncovered that miR-541-3p had a negative relationship with LINC00638 in NSCLC tissues (Fig. 3E). Additionally, the outcomes of dual luciferase reporter gene assay displayed that miR-541-3p mimics inhibited LINC00638-WT's luciferase activity, while it exerted no obvious impact on LINC00638-MT luciferase activity (Fig. 3F). In addition, the RIP experiments established the association between LINC00638 and miR-541-3p (Fig. 3G), and KM plotter analysis indicated that low miR-541-3p levels exhibited a correlation with the poorer overall survival of NSCLC patients (Fig. 3H). All in all, LINC00638 targeted miR-541-3p and restricted its profile.

3.4. miR-541-3p inhibited NSCLC development in vitro

The overexpression and knockdown models of miR-541-3p were built in HCC-827 and H460 (Fig. 4A and B). As per the outcomes of CCK-8 and colony formation assays, cell proliferation and colony formation ability were reduced subsequent to overexpression of miR-541-3p, while they were notably enhanced after miR-541-3p knockdown (Fig. 4C–E). Furthermore, cell apoptosis was increased following miR-541-3p mimics transfection, while it was decreased subsequent to transfection with the miR-541-3p inhibitors (Fig. 4 F). Western blot reflected that up-regulating miR-541-3p mitigated cyclin D1, cyclin E1, CDK2, and CDK4 levels and enhanced p21 and p27 levels, while downregulating miR-541-3p exhibited the reverse effects (Fig. 4 G). Moreover, Transwell assay denoted that miR-

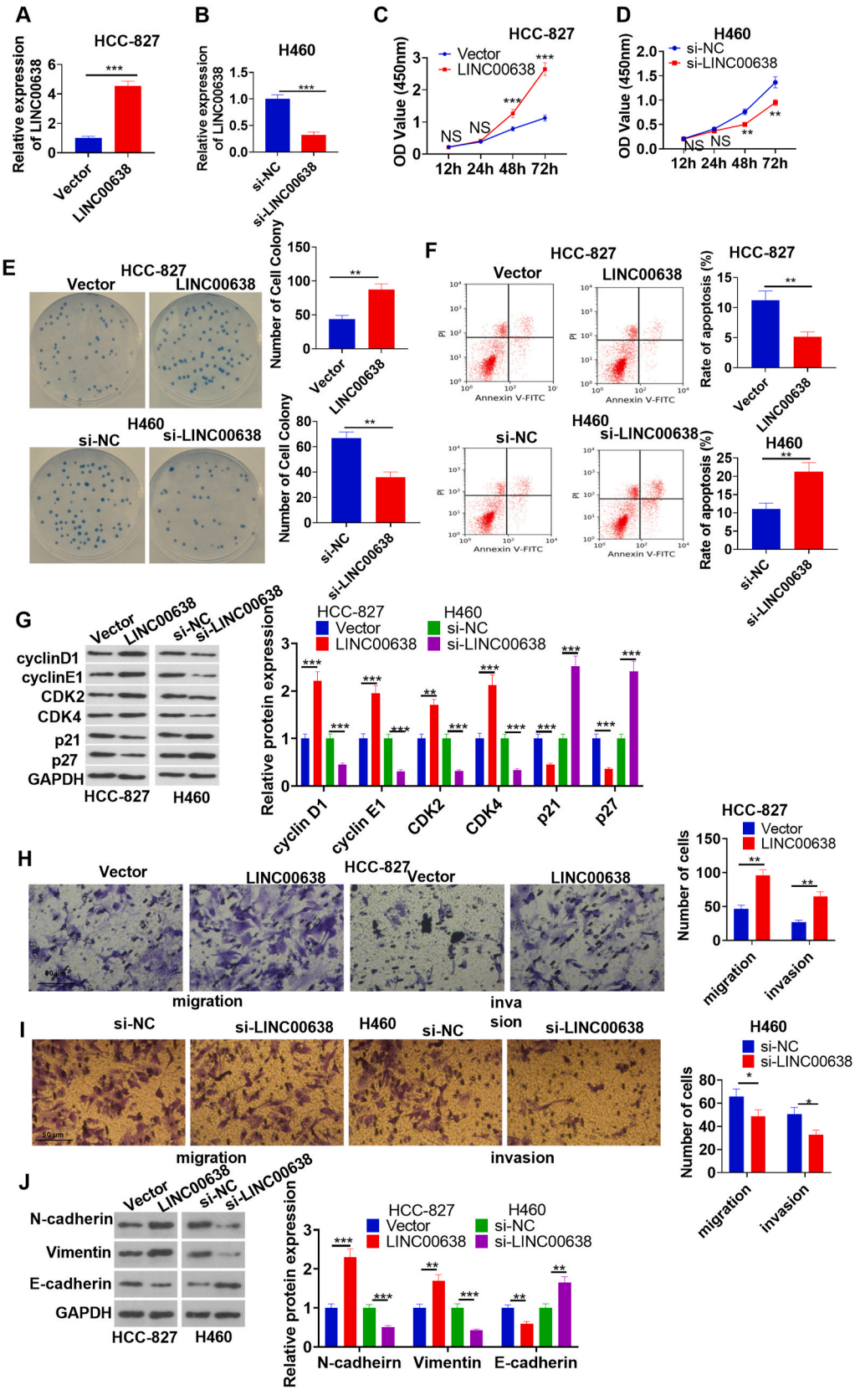

(caption on next page)

Fig. 2. The influence of LINC00638 progression A and B: An LINC00638 overexpression or downregulation model was constructed in NSCLC cell line HCC-827(A) and H460 (B) cells, respectively. ***$P < 0.001$. C and D: HCC-827 (C) and H460 (D) proliferation measured by CCK-8. *P < 0.05, **$P < 0.01$, ***$P < 0.001$ (vs. Vector or si-NC). E: HCC-827 and H460 cell colony formation evaluated through colony formation assay. F: HCC-827 and H460 cell apoptosis monitored by flow cytometry. G: Proteins associated with cell cycle (cyclin D, cyclin E, CDK2 CDK4, p21, p27) in HCC-827 and H460 detected by Western blot. H and I: HCC-827 and H460 cell migration and invasion investigated by Transwell. J. HCC-827 and H460 cell EMT were determined using Western blot (for detecting E-cadherin, Vimentin, and N-cadherin). *P < 0.01, **P < 0.01, ***P < 0.01. n = 3.

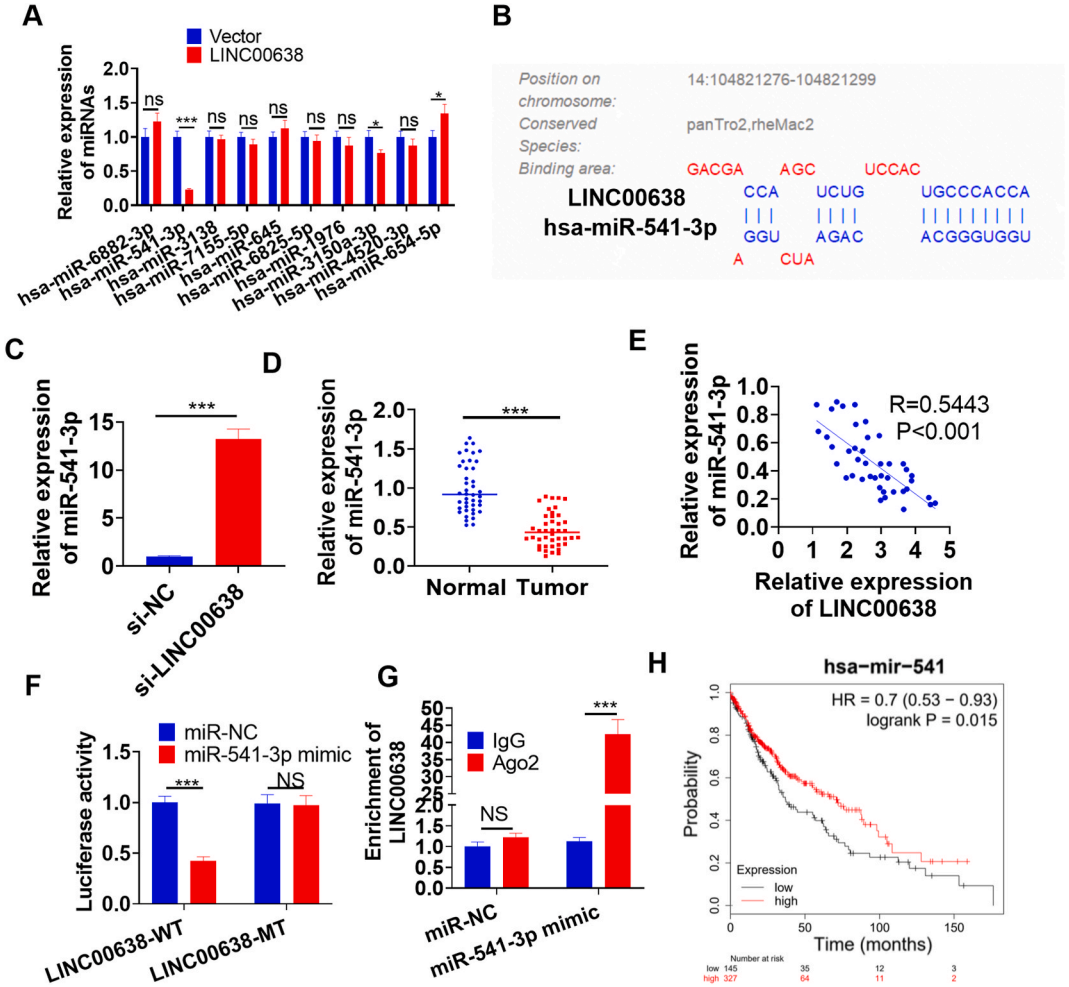

Fig. 3. The interaction between LINC00638 and miR-541-3p in NSCLC cells. A: The profiles of the candidate target miRNAs of LINC00638 were determined by RT-PCR. B: ENCORI (http://carolina.imis.athena-innovation.gr/diana_tools/web/index.php) predicted that LINC00638 contained binding sites with miR-541-3p. C. miR-541-3p expression in LINC00638-overexpressed HCC-827 cells was verified by RT-PCR. D: The miR-541-3p level in NSCLC tissues and adjacent normal tissues was checked through RT-PCR. E: The relationship between LINC00638 and miR-541-3p expressions was analyzed by Pearson. $R^2 = 0.5443$, $P < 0.0001$. F: The binding association between miR-541-3p and LINC00638 was confirmed by dual luciferase reporter gene assay. G. RIP was conducted. LINC00638 enrichment in the immunoprecipitated RNA was detected by RT-PCR. H. The affinity between miR-541-3p and the overall survival of lung cancer was evaluated by KM plotter (https://www.jianshu.com/p/49ceeae7fd95). NS P > 0.05, ***P < 0.001. n = 3.

541-3p overexpression showed an inhibitory impact on NSCLC cell migration and invasion (Fig. 4H–I). The data of Western blot confirmed that miR-541-3p repressed the EMT of NSCLC cells (Fig. 4 J). The aforementioned results demonstrated that miR-541-3p correlated with the malignant phenotype of NSCLC and might act as a tumor-suppressing gene.

3.5. miR-541-3p reversed the impact of LINC00638

miR-541-3p mimics were transfected into LINC00638-overexpressing HCC-827 cells for the purpose of ascertaining the function of the LINC00638/miR-541-3p axis in regulating NSCLC development. RT-PCR showed that overexpressing LINC00638 induced miR-

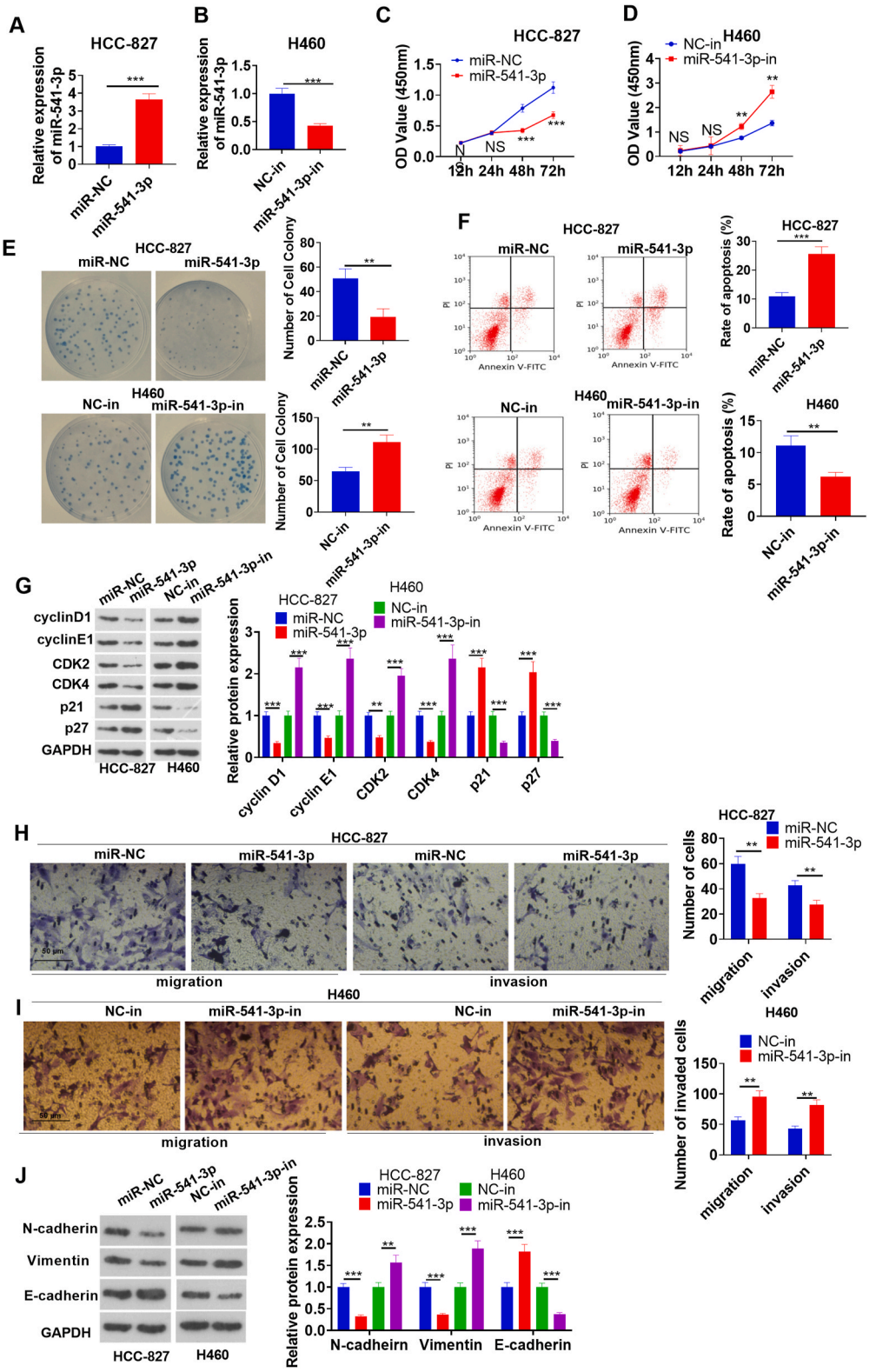

Fig. 4. The influence of miR-541-3p on NSCLC cell proliferation, apoptosis and metastasis. A and B: An miR-541-3p overexpression or knockdown model was constructed in NSCLC cell line HCC-827(A) and H460 (B) cells, respectively. The miR-541-3p level was checked by RT-PCR. ***$P < 0.001$. C and D: HCC-827 (C) and H460 (D) proliferation was evaluated by CCK-8. NS, $P > 0.05$, *$P < 0.05$, **$P < 0.01$, ***$P < 0.001$ (vs. miR-NC or miR-in). E: HCC-827 and H460 cell colony formation was monitored through colony formation assay. F: HCC-827 and H460 cell

apoptosis was checked by flow cytometry. G. cyclin D, cyclin E, CDK2 CDK4, p21, and p27 proteins in HCC-827 and H460 were monitored through Western blot. H and I: HCC-827 and H460 cell migration and invasion were assessed by Transwell. J: HCC-827 and H460 cell EMT was examined by Western blot (for detecting E-cadherin, Vimentin, and N-cadherin). *P < 0.05, **P < 0.01, ***P < 0.001. n = 3.

541-3p downregulation, whereas miR-541-3p mimics transfection enhanced the miR-541-3p level (Fig. 5A and B). Functional assays showed that cell proliferation, colony formation, migration, invasion, and EMT were markedly downregulated in the group of LINC00638+miR-541-3p vis-à-vis the group of LINC00638, while cell apoptosis was significantly enhanced after miR-541-3p overexpression (Fig. 5C–H). The aforementioned outcomes suggested that miR-541-3p reversed the malignant behaviors of HCC-827 cells with LINC00638 overexpression.

3.6. miR-541-3p targeted IRS1

For exploring the targets and mechanism of miR-541-3p, 43 genes were found sharing in microT, mipmap, Targetscan and Genecards using Venny's diagram analysis (sup figure A). Gene function enrichment analysis showed that those targets were enriched in regulating several KEGG pathways, such as Pathways in cancer, Regulation of actin cytoskeleton, Neurotrophin signaling pathway,

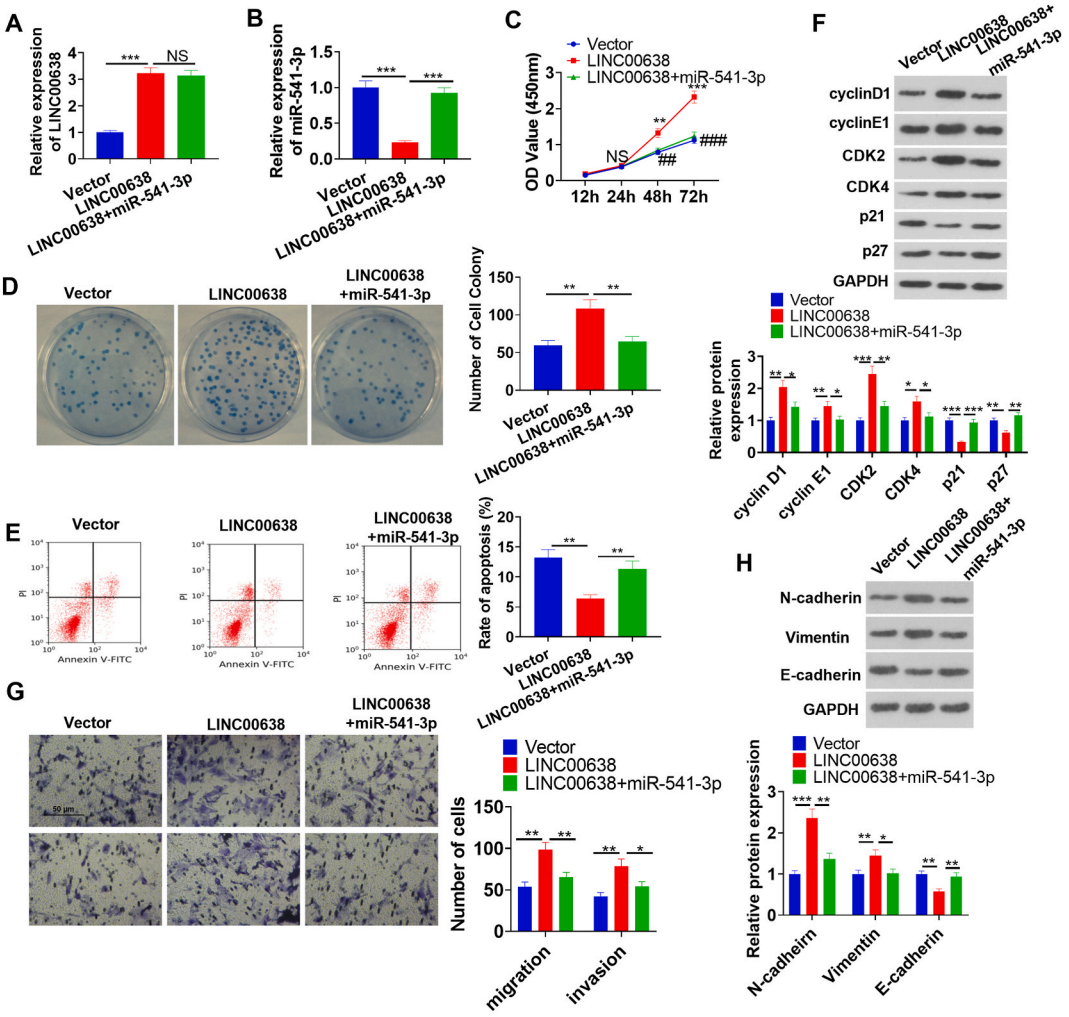

Fig. 5. The regulatory influence of LINC00638/miR-541-3p on NSCLC. LINC00638-overexpressed HCC-827 cells were transfected together with miR-541-3p mimics. A and B: LINC00638 (A) and miR-541-3p (B) levels verified via RT-PCR. C: HCC-827 cell proliferation was examined by CCK-8. NS, **P < 0.01, ***P < 0.001 (vs. vector); ##P < 0.01, ###P < 0.001 (vs. LINC00638); D. HCC-827 and H460 cell colony formation was checked by colony formation experiment. E: HCC-827 and H460 cell apoptosis was evaluated by flow cytometry. F: Proteins related to cell cycle (cyclin D, cyclin E, CDK2 CDK4, p21, p27) in HCC-827 and H460 were monitored through Western blot. G: HCC-827 and H460 cell migration and invasion were assessed by Transwell. H: HCC-827 and H460 cell EMT was examined by Western blot (for detecting E-cadherin, Vimentin, and N-cadherin). NS P > 0.05, *P < 0.05, **P < 0.01, ***P < 0.001. n = 3.

Breast cancer, Gastric cancer, Hippo signaling pathway, Hepatocellular carcinoma et al. (sup figure B), and affect Gene Ontology (GO) items, such as focal adhesion, actin cytoskeleton, negative regulation of cell proliferation (sup figure C). StarBase (http://starbase.sysu.edu.cn/) discovered three binding sites for miR-541-3p in IRS1 mRNA (Fig. 6A). Next, dual luciferase reporter gene assay confirmed that miR-541-3p targeted the 3′-UTR of IRS1 mRNA (Fig. 6B). Western blot checked the levels of IRS1, PI3K and Akt after selectively regulating LINC00638 and miR-541-3p. The results exhibited that overexpressing LINC00638 or inhibiting miR-541-3p significantly promoted IRS1, p-PI3K and p-Akt expressions, whereas LINC00638 knockdown or miR-541-3p upregulation produced the opposite phenomenon (Fig. 6E–F). Moreover, rescue experiments showed that miR-541-3p repressed IRS1, p-PI3K and p-Akt expression, which were promoted following LINC00638 overexpression (Fig. 6 G). Overall, LINC00638/miR-541-3p axis has a regulatory role on IRS1/PI3K/Akt pathway.

3.7. *Inhibiting IRS1 attenuated LINC00638-mediated promotive effects on NSCLC cells*

For confirming the role of IRS1 in LINC00638-mediated promotive effects on NSCLC cells, the IRS1/2 inhibitor NT157 was administered into HCC-827 cells with LINC00638 upregulation. We found that NR157 had no significant effects on LINC00638 and miR-541-3p expression (Fig. 7A–B). HCC-827 cell proliferation and colony formation were tested. When contrasted to the LINC00638 group, NT157 repressed the proliferative and colonic abilities of HCC-827 cells (Fig. 7C–D). What is more, flow cytometry and Western blot verified that NT157 dampened cyclin D1, cyclin E1, CDK2, and CDK4 profiles and enhanced p21 and p27 expressions as well as cell apoptosis ($p < 0.05$ vs. LINC00638 group, Fig. 7E–F). As evidenced by Transwell and Western blot, NT157 exhibited an inhibitory impact on the migration, invasion, and EMT of NSCLC cells (Fig. 7G–H). The IRS1/PI3K/AKT pathway was significantly inhibited with NT157 treatment (Fig. 7 I). Collectively, those data supported that NT157 attenuated LINC00638-mediated oncogenic effects.

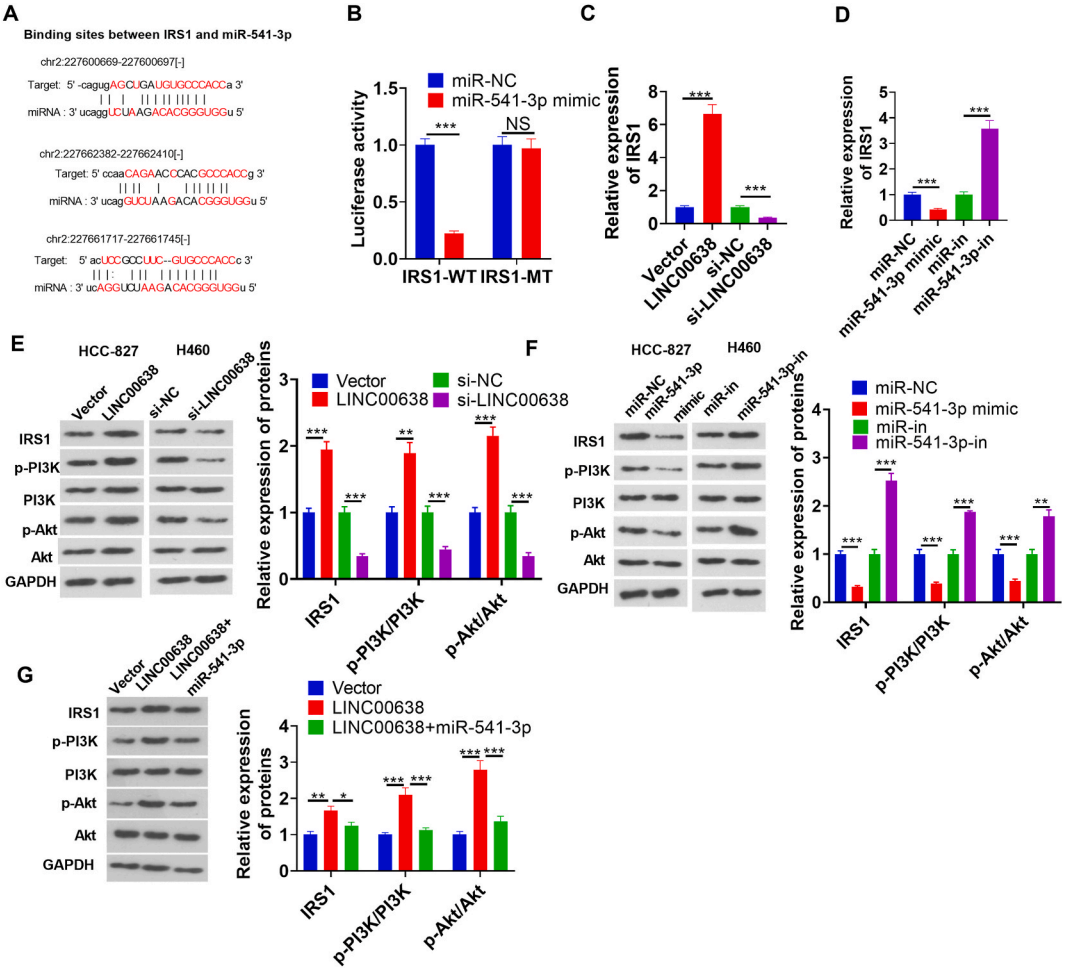

Fig. 6. IRS1 was a functional target of miR-541-3p in NSCLC cells. A: The binding sites of IRS1 mRNA with miR-541-3p were predicted through Starbase. B: The relevance between IRS1 and miR-541-3p was examined through dual luciferase reporter gene assay. C–D: The IRS1 mRNA level in NSCLC cells detected by RT-PCR. E-G. IRS1, PI3K, and Akt expressions were confirmed by Western blot after selectively regulating LINC00638 and miR-541-3p. NS $P > 0.05$, *$P < 0.05$, **$P < 0.01$, ***$P < 0.001$. $n = 3$.

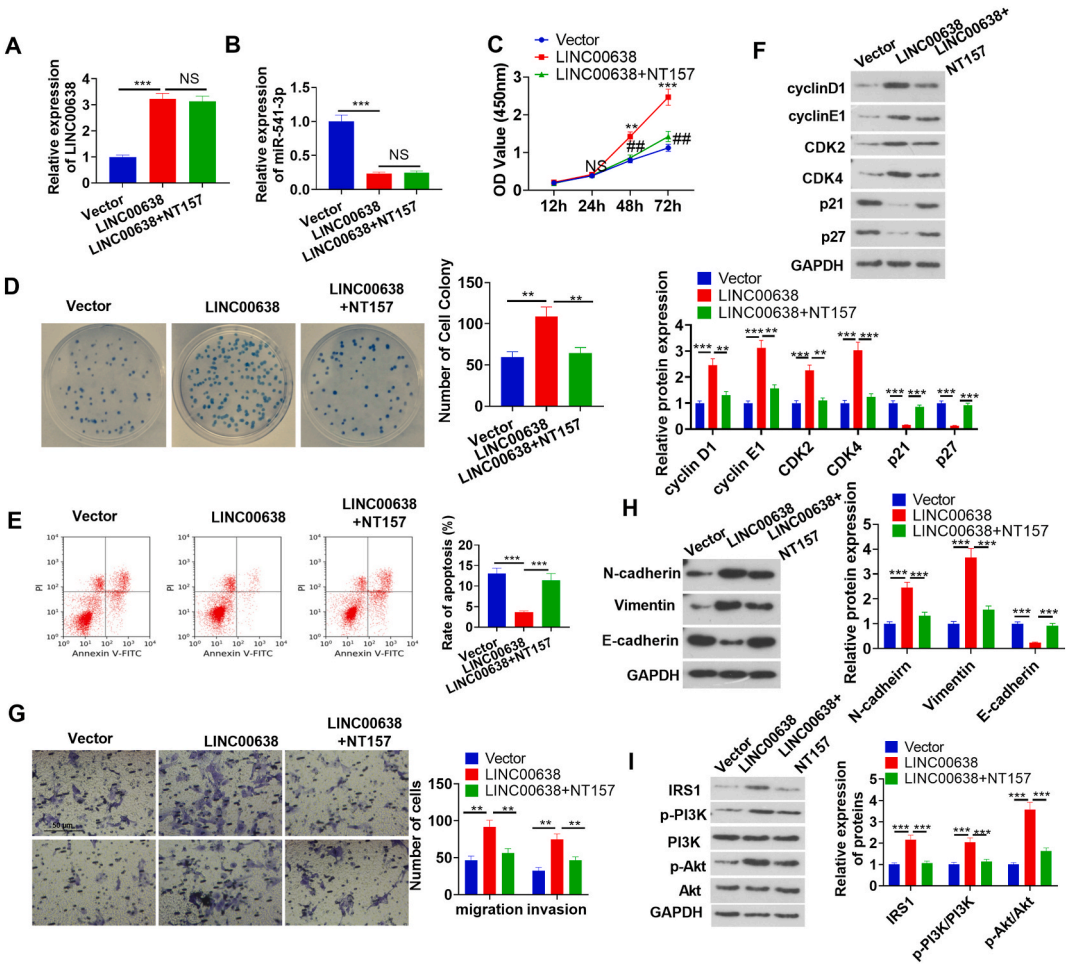

Fig. 7. Inhibiting IRS1 reversed the promotive effect of LINC00638 on NSCLC. LINC00638-overexpressed HCC-827 cells were treated with the IRS1/2 inhibitor NT157. A and B: LINC00638 (A) and miR-541-3p (B) levels were verified by RT-PCR. C: HCC-827 cell proliferation was monitored through CCK-8 assay. NS, **P < 0.01, ***P < 0.001 (vs. vector); ##P < 0.01, ###P < 0.001 (vs. LINC00638); D: HCC-827 and H460 cell colony formation was checked by colony formation assay. E: HCC-827 and H460 cell apoptosis was tracked by flow cytometry. F: Proteins related to cell cycle (cyclin D, cyclin E, CDK2 CDK4, p21, p27) in HCC-827 and H460 were monitored through Western blot. G: HCC-827 and H460 cell migration and invasion were evaluated by employing Transwell. H: HCC-827 and H460 cell EMT was gauged by Western blot (for detecting E-cadherin, Vimentin, and N-cadherin). I: IRS1, PI3K and Akt levels were confirmed via Western blot. NS P > 0.05, *P < 0.05, **P < 0.01, ***P < 0.001. n = 3.

3.8. LINC00638 enhanced HCC-827 growth in vivo by altering the miR-541-3p- IRS1/PI3K/AKT axis

A Xenograft model was constructed in nude mice for evaluating the LINC00638-mediated impact on NSCLC cell growth. It was found that HCC-827 cells with LINC00638 upregulation exhibited enhanced growth ability ($p < 0.01$, Fig. 8A–C). By performing IHC, we found that LINC00638 promoted Vimentin, IRS1, p-AKT level, and repressed E-cadherin (Fig. 8D). RT-PCR results showed that LINC00638, as well as IRS1/PI3K/AKT pathway, were significantly increased in LINC00638 group, whereas miR-541-3p was inhibited ($P < 0.01$ vs. vector group, Fig. 8E–G). Taken together, we believed that LINC00638 promoted HCC-827 cell growth in vivo by altering the miR-541-3p- IRS1/PI3K/AKT axis.

4. Discussion

Our research revealed that the LINC00638 level was dramatically heightened in NSCLC tissues and cells. Furthermore, LINC00638 bolstered cell proliferation and invasion and dampened apoptosis, indicating that LINC00638 regulates the miR-541-3p-mediated IRS1/PI3K/AKT axis so as to exert a carcinogenic function in NSCLC.

Numerous studies have reported that lncRNAs exhibit significantly differentiated profiles in lung cancer, which affects lung cancer development in various ways [20]. For example, lncRNA MBNL1-AS1 was uncovered to be downregulated in NSCLC tissues, while overexpressing MBNL1-AS1 attenuated NSCLC tumorigenesis [21]. In addition, overexpressing lncRNA GAS5 aggravated ionizing radiation-induced apoptosis of A549 cells through modulation of the miR-21/phosphatase and tensin homolog/Akt axis [22].

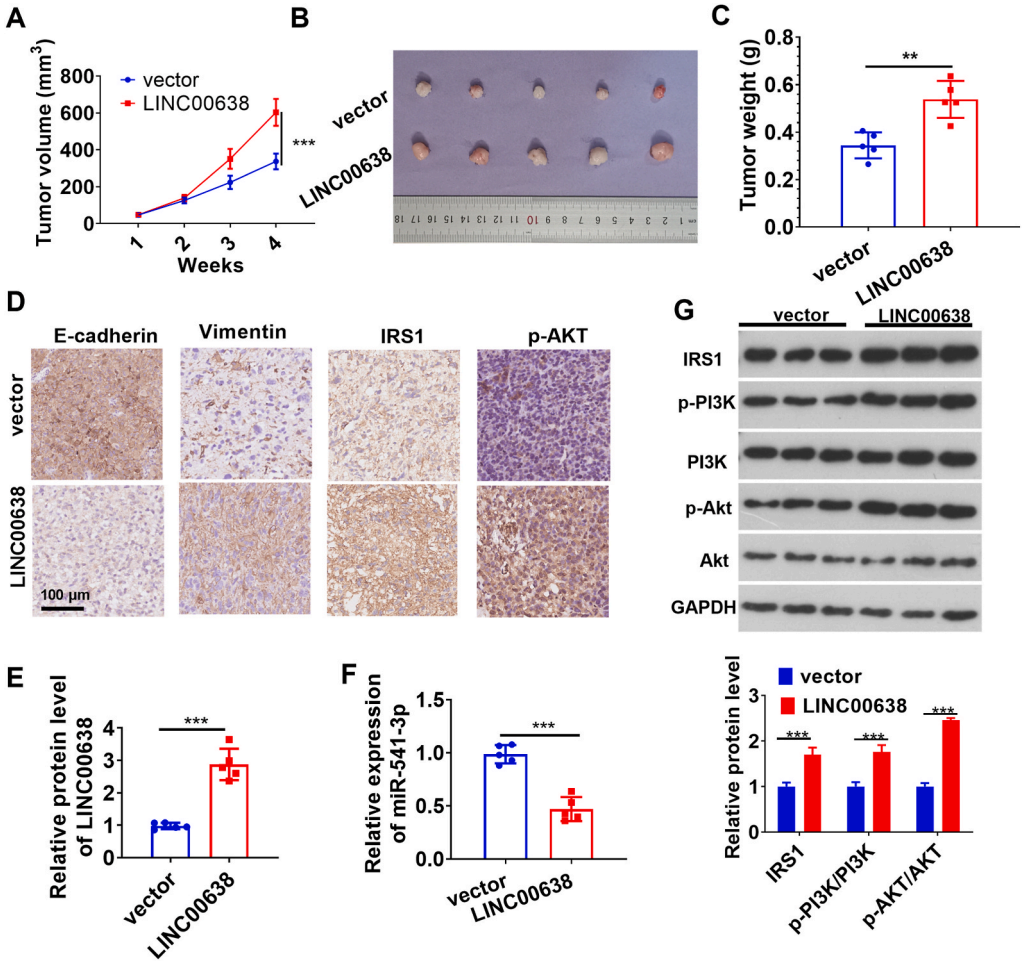

Fig. 8. LINC00638 bolstered NSCLC cell growth. LINC00638-overexpressed HCC-827 cells were adopted for building a xenograft model in nude mice for evaluating the role of LINC00638 in NSCLC cell growth. A: The tumor volume was calculated every week. B–C: The tumors were isolated and weighed during the 4th week after the construction of the HCC-827 cell xenograft. D: The protein levels of E-cadherin, Vimentin, IRS1, and p-AKT in the tumors were detected by IHC. E–G: LINC00638, miR-541-3p, and the IRS1/PI3K/AKT pathway in the tumors evaluated through RT-PCR and Western blot. $^{**}P < 0.01$, $^{***}P < 0.001$. n = 5.

Furthermore, LINC00958, which is induced by its promoter SP1, can amplify lung adenocarcinoma cell proliferation, migration, and invasion by modulating the miR-625-5p/CPSF7 axis [23]. Recently, LINC00638 has been demonstrated to potentially affect NK cell infiltration in hepatocellular carcinoma (HCC) with high tumor mutation burden (TMB) by targeting the miR-4732-3p/ULBP1 axis [14]. This study probed the function of the novel lncRNA LINC00638 during NSCLC progression. The data revealed that LINC00638 was upregulated in NSCLC tissues, might serve as a predictor of poorer survival of patients with NSCLC, significantly increased the proliferation, colony formation ability, migration, and invasion, and inhibited the apoptosis of NSCLC cells, indicating that LINC00638 was implicated in NSCLC occurrence and progression as an oncogene.

In addition to lncRNAs, miRNAs also participate in lung cancer progression via modulating apoptosis, growth, metastasis, and chemotherapy resistance. For example, increased miR-196b expression boosts lung cancer cell migration and invasion in a TSPAN12 and GATA6-dependent pattern [24]. In addition, miR-212-5p exhibits a promotive function by targeting the Id3/PI3K/Akt axis in lung adenocarcinoma cells [25]. LncRNA functions as a competitive endogenous RNA (ceRNA) via sponging miRNA, thus indirectly inducing gene dysregulation. For example, TMPO-AS1 bolsters lung adenocarcinoma development and is negatively modulated by miR-383-5p [26]. Additionally, lncRNA NORAD may regulate lung cancer cell proliferation, apoptosis, migration, and invasion by way of the miR-30a-5p/ADAM19 axis [27]. miR-541-3p is an annotated microRNA listed in miRbase (https://www.mirbase.org/), and our analysis based on the miRNA-lncRNA interaction networks via ENCORI (https://starbase.sysu.edu.cn/index.php) showed that [28] miR-541-3p was a promising target of LINC00638. Further experiments verified that LINC00638 sponged miR-541-3p so as to function as a ceRNA. Thus, gain- and loss-of-function of miR-541-3p assays were conducted, and it was found that mir-541-3p exerted significant anticancer effects on NSCLC. Furthermore, overexpressing miR-541-3p vigorously suppressed the carcinogenic effects of LINC00638. Therefore, LINC00638 might promote NSCLC progression via sponging miR-541-3p, a tumor inhibitor in NSCLC. However, the TargetScan Human (https://www.targetscan.org/vert_72/), one of the most respected microRNA-to-target prediction

databases conducted by David Bartel laboratory at MIT [29], indicates that hsa-miR-541-3p is not confidently annotated but shares a seed with the following confidently annotated family and thus has the same predicted targets of miR-654-5p. This might be caused by the different prediction mechanisms of different databases.

For investigating the downstream mechanism of miR-541-3p, we performed bioinformatics analysis for analyzing the downstream targets and mechanism of miR-541-3p. 43 targets were identified as the potential targets miR-541-3 and they were enriched in regulating several KEGG pathways, such as Pathways in cancer, Regulation of actin cytoskeleton, Neurotrophin signaling pathway, Breast cancer, Gastric cancer, Hippo signaling pathway, Hepatocellular carcinoma et al., and affect Gene Ontology (GO) items, such as focal adhesion, actin cytoskeleton, negative regulation of cell proliferation. Those pathways and GO items are involved in cancer progression. IRS1 is one target gene among those 43 targets. A previous study has revealed that IRS1 is a critical regulator in the insulin signaling pathway and is phosphorylated by insulin receptor tyrosine kinase. Mutation of IRS1 has a relation to type II diabetes and susceptibility to insulin resistance [30,31]. Moreover, IRS1 functioned as an essential therapeutic target of NSCLC [32,33], and it is involved in the Neurotrophin signaling pathway, which includes the PI3K-AKT axis [34–36]. The present study identified IRS1 as a target of miR-541-3p and verified that LINC00638 increased IRS1 expression in NSCLC cells, which was inhibited by miR-541-3p. Therefore, the LINC00638/miR-541-3p axis might affect NSCLC progression via IRS1.

PI3K, belonging to the intracellular lipid kinase family, takes part in the modulation of cellular proliferation, differentiation and survival [37]. The PI3K/Akt pathway has been considered as a classical signaling pathway with a crucial function in regulating malignant behaviors, like cell proliferation, cell cycle progression, metastasis, apoptosis, drug resistance, and stemness [38–41]. Increasing preclinical and clinical evidence has been found in terms of specific inhibitors of the PI3K/Akt pathway in treating cancer [42]. The PI3K/Akt pathway, a classical signaling pathway involved in most cancer types, can also be activated by IRS1 [43]. Notably, this protein-protein regulatory mechanism serves as a target in cancer therapy. For example, targeting the insulin-like growth factor 1 (IGF1R)/IRS1 axis exerts cytotoxic effects through inhibiting PI3K/Akt/mammalian target of rapamycin and MAPK signaling in acute lymphoblastic leukemia cells [44]. In NSCLC, Wentilactone A induces apoptosis of NSCLC cells by targeting the AKR1C1 gene via the IGF1R/IRS1/PI3K/Akt/nuclear factor erythroid 2-related factor 2/FLICE-like inhibitory protein/caspase-3 signaling pathway [45]. Collectively, those studies have all displayed that the IRS1/PI3K/Akt axis had a crucial regulatory role in cancer. Here, we discovered that LINC00638 increased the IRS1/PI3K/Akt expression in NSCLC cells, whereas miR-541-3p inhibited the axis. Thus, LINC00638 and miR-541-3p functioned as regulators in NSCLC, at least partly by modulating IRS1/PI3K/Akt.

However, several limitations are required for further exploration in the further study. First, more clinical samples are needed for confirming the diagnostic value and outcome prediction value of LINC00638-miR-541-3p/IRS1 in NSCLC. Second, the mechanistic part solely relies on two NSCLC cell lines, and the *in-vivo* assays have only confirmed the oncogenic role of LINC00638 in one lung cancer cell, representing tumor clones rather than the complex picture of NSCLC seen in the clinic. Third, the presented data lacks an integral exploration of the LINC00638-miR-541-3p/IRS1/PI3K/Akt axis in the progression of NSCLC. Forth, NSCLC represents numerous diseases that may be targeted by chemotherapy, immune checkpoint inhibitors, or targeted therapies (e.g., TKIs against EGFR or ALK) depending on the molecular landscape [46,47]. While the proposed lncRNA, miR-541-3p, and IRS1 seemingly have potential in the demonstrated *in vitro* cultures, it remains to be seen whether any of these factors would play a role in more sophisticated models such as patient-derived xenograft models.

Overall, the above statistics confirmed that LINC00638 overexpression targeted the miR-541-3p/IRS1/PI3K/Akt axis, hence promoting NSCLC development. Our research offers novel insights into the molecular target therapy of NSCLC.

Declarations

Ethics approval statement

Our study was approved by the Ethics Review Board of Xiangyang Central Hospital, Affiliated Hospital of Hubei University of Arts and Science.

Author contribution statement

Juan Zhang: Performed the experiments; Contributed reagents, materials, analysis tools or data; Wrote the paper.
Yanhua Mou: Performed the experiments; Wrote the paper.
Hui Li: Performed the experiments; Analyzed and interpreted the data.
Hui Shen; Jun Song: Analyzed and interpreted the data; Contributed reagents, materials, analysis tools or data.
Qingfeng Li: Conceived and designed the experiments.

Data availability statement

Data will be made available on request.

Declaration of competing interest

The authors declare that they have no known competing financial interests or personal relationships that could have appeared to influence the work reported in this paper.

Appendix A. Supplementary data

Supplementary data to this article can be found online at https://doi.org/10.1016/j.heliyon.2023.e16999.

References

[1] R.L. Siegel, K.D. Miller, A. Jemal, Cancer statistics, 2019, CA A Cancer J. Clin. 69 (1) (2019) 7–34.
[2] N. Duma, R. Santana-Davila, J.R. Molina, Non-small cell lung cancer: epidemiology, screening, diagnosis, and treatment, Mayo Clin. Proc. 94 (8) (2019) 1623–1640.
[3] B.C. Gulack, M.L. Cox, C.J. Yang, et al., Survival after radiation for stage I and II non-small cell lung cancer with positive margins, J. Surg. Res. 223 (2018) 94–101.
[4] Z. Pan, K. Wang, X. Wang, et al., Cholesterol promotes EGFR-TKIs resistance in NSCLC by inducing EGFR/Src/Erk/SP1 signaling-mediated ERRα re-expression, Mol. Cancer 21 (1) (2022) 77.
[5] M. Yuan, L.L. Huang, J.H. Chen, J. Wu, Q. Xu, The emerging treatment landscape of targeted therapy in non-small-cell lung cancer, Signal Transduct. Targeted Ther. 4 (2019) 61.
[6] A. Passaro, J. Brahmer, S. Antonia, T. Mok, S. Peters, Managing resistance to immune checkpoint inhibitors in lung cancer: treatment and novel strategies, J. Clin. Oncol. 40 (6) (2022) 598–610.
[7] K. Taniue, N. Akimitsu, The functions and unique features of LncRNAs in cancer development and tumorigenesis, Int. J. Mol. Sci. 22 (2) (2021) E632.
[8] Y. Xu, M. Qiu, M. Shen, et al., The emerging regulatory roles of long non-coding RNAs implicated in cancer metabolism, Mol. Ther. 29 (7) (2021) 2209–2218.
[9] S. Li, Y. Cao, H. Zhang, et al., Construction of lncRNA-mediated ceRNA network for investigating immune pathogenesis of ischemic stroke, Mol. Neurobiol. 58 (9) (2021) 4758–4769.
[10] K. Su, N. Wang, Q. Shao, H. Liu, B. Zhao, S. Ma, The role of a ceRNA regulatory network based on lncRNA MALAT1 site in cancer progression, Biomed. Pharmacother. 137 (2021), 111389.
[11] Y. Zhao, D. Zhou, Y. Yuan, et al., MAPKAPK5-AS1/miR-515-5p/CAB39 Axis contributes to non-small cell lung cancer cell proliferation and migration, Mol. Biotechnol. (2023), https://doi.org/10.1007/s12033-023-00654-w.
[12] L. Zhang, X.F. Zhou, G.F. Pan, J.P. Zhao, Enhanced expression of long non-coding RNA ZXF1 promoted the invasion and metastasis in lung adenocarcinoma, Biomed. Pharmacother. 68 (4) (2014) 401–407.
[13] Y.H. Zhang, J. Song, L. Shen, J. Shao, Systematic identification of lncRNAs and circRNAs-associated ceRNA networks in human lumbar disc degeneration, Biotech. Histochem. 94 (8) (2019) 606–616.
[14] F. Qi, X. Du, Z. Zhao, et al., Tumor mutation burden-associated LINC00638/miR-4732-3p/ULBP1 Axis promotes immune escape via PD-L1 in hepatocellular carcinoma, Front. Oncol. 11 (2021), 729340.
[15] S. Chen, Y. Wang, D. Li, et al., Mechanisms controlling MicroRNA expression in tumor, Cells 11 (18) (2022) 2852.
[16] E.V. Semina, K.D. Rysenkova, K.E. Troyanovskiy, A.A. Shmakova, K.A. Rubina, MicroRNAs in cancer: from gene expression regulation to the metastatic niche reprogramming, Biochemistry (Mosc.) 86 (7) (2021) 785–799.
[17] A. Ahadi, Dysregulation of miRNAs as a signature for diagnosis and prognosis of gastric cancer and their involvement in the mechanism underlying gastric carcinogenesis and progression, IUBMB Life (2020), https://doi.org/10.1002/iub.2259.
[18] H. Meng, B. Li, W. Xu, et al., miR-140-3p enhances the sensitivity of LUAD cells to antitumor agents by targeting the ADAM10/Notch pathway, J. Cancer 13 (15) (2022) 3660–3673.
[19] B. Long, N. Li, X.X. Xu, et al., Long noncoding RNA LOXL1-AS1 regulates prostate cancer cell proliferation and cell cycle progression through miR-541-3p and CCND1, Biochem. Biophys. Res. Commun. 505 (2) (2018) 561–568.
[20] S. Talebi, A.J. Abadi, G. Kazemioula, et al., Expression analysis of five different long non-coding ribonucleic acids in nonsmall-cell lung carcinoma tumor and tumor-derived exosomes, Diagnostics 12 (12) (2022) 3209.
[21] G. Cao, B. Tan, S. Wei, et al., Down-regulation of MBNL1-AS1 contributes to tumorigenesis of NSCLC via sponging miR-135a-5p [published online ahead of print, 2020 Feb 19], Biomed. Pharmacother. 125 (2020), 109856.
[22] L. Chen, P. Ren, Y. Zhang, B. Gong, D. Yu, X. Sun, Long non-coding RNA GAS5 increases the radiosensitivity of A549 cells through interaction with the miR-21/PTEN/Akt axis, Oncol. Rep. 43 (3) (2020) 897–907.
[23] L. Yang, L. Li, Z. Zhou, et al., SP1 induced long non-coding RNA LINC00958 overexpression facilitate cell proliferation, migration and invasion in lung adenocarcinoma via mediating miR-625-5p/CPSF7 axis, Cancer Cell Int. 20 (2020) 24.
[24] G. Liang, W. Meng, X. Huang, et al., miR-196b-5p-mediated downregulation of TSPAN12 and GATA6 promotes tumor progression in non-small cell lung cancer, Proc. Natl. Acad. Sci. U. S. A. (2020), 201917531.
[25] F.F. Chen, N. Sun, Y. Wang, et al., miR-212-5p exerts tumor promoter function by regulating the Id3/PI3K/Akt axis in lung adenocarcinoma cells [published online ahead of print, 2020 Feb 10], J. Cell. Physiol. (2020), https://doi.org/10.1002/jcp.29627.
[26] X. Mu, H. Wu, J. Liu, et al., Long noncoding RNA TMPO-AS1 promotes lung adenocarcinoma progression and is negatively regulated by miR-383-5p [published online ahead of print, 2020 Feb 13], Biomed. Pharmacother. 125 (2020), 109989.
[27] J. Li, X. Xu, C. Wei, L. Liu, T. Wang, Long noncoding RNA NORAD regulates lung cancer cell proliferation, apoptosis, migration, and invasion by the miR-30a-5p/ADAM19 axis, Int. J. Clin. Exp. Pathol. 13 (1) (2020) 1–13.
[28] J.H. Li, S. Liu, H. Zhou, L.H. Qu, J.H. Yang, starBase v2.0: decoding miRNA-ceRNA, miRNA-ncRNA and protein-RNA interaction networks from large-scale CLIP-Seq data, Nucleic Acids Res. 42 (Database issue) (2014) D92–D97.
[29] V. Agarwal, G.W. Bell, J.W. Nam, D.P. Bartel, Predicting effective microRNA target sites in mammalian mRNAs, Elife 4 (2015), e05005.
[30] Jun Zhou, Kaixun Huang, Peroxynitrite mediates muscle insulin resistance in mice via nitration of IRbeta/IRS-1 and Akt, Toxicol. Appl. Pharmacol. 241 (2009) 101–110.
[31] Yafan Gong, Jie Yang, Liu Qi, et al., IGF1 knockdown hinders myocardial development through energy metabolism dysfunction caused by ROS-dependent FOXO activation in the chicken heart, Oxid. Med. Cell. Longev. 2019 (2019), 7838754.
[32] H. Xu, M.S. Lee, P.Y. Tsai, et al., Ablation of insulin receptor substrates 1 and 2 suppresses Kras-driven lung tumorigenesis, Proc. Natl. Acad. Sci. U. S. A. 115 (16) (2018) 4228–4233.
[33] A.J. Piper, J.L. Clark, J. Mercado-Matos, et al., Insulin Receptor Substrate-1 (IRS-1) and IRS-2 expression levels are associated with prognosis in non-small cell lung cancer (NSCLC), PLoS One 14 (8) (2019), e0220567.
[34] J. Jiang, J. Bai, T. Qin, Z. Wang, L. Han, NGF from pancreatic stellate cells induces pancreatic cancer proliferation and invasion by PI3K/AKT/GSK signal pathway, J. Cell Mol. Med. 24 (10) (2020) 5901–5910.
[35] Y. Yuan, H.Q. Ye, Q.C. Ren, Proliferative role of BDNF/TrkB signaling is associated with anoikis resistance in cervical cancer, Oncol. Rep. 40 (2) (2018) 621–634.
[36] Y.F. Tsai, L.M. Tseng, C.Y. Hsu, M.H. Yang, J.H. Chiu, Y.M. Shyr, Brain-derived neurotrophic factor (BDNF) -TrKB signaling modulates cancer-endothelial cells interaction and affects the outcomes of triple negative breast cancer, PLoS One 12 (6) (2017), e0178173.
[37] J.S. Yu, W. Cui, Proliferation, survival and metabolism: the role of PI3K/AKT/mTOR signalling in pluripotency and cell fate determination, Development 143 (17) (2016) 3050–3060.

[38] J.S. Liu, C.Y. Huo, H.H. Cao, et al., Aloperine induces apoptosis and G2/M cell cycle arrest in hepatocellular carcinoma cells through the PI3K/Akt signaling pathway, Phytomedicine 61 (2019), 152843.
[39] H. Chen, L. Zhou, X. Wu, et al., The PI3K/AKT pathway in the pathogenesis of prostate cancer, Front. Biosci. 21 (2016) 1084–1091.
[40] Y. Li, Y. Guo, Z. Feng, et al., Involvement of the PI3K/Akt/Nrf2 signaling pathway in resveratrol-mediated reversal of drug resistance in HL-60/ADR cells, Nutr. Cancer 71 (6) (2019) 1007–1018.
[41] J. Chen, R. Shao, F. Li, et al., PI3K/Akt/mTOR pathway dual inhibitor BEZ235 suppresses the stemness of colon cancer stem cells, Clin. Exp. Pharmacol. Physiol. 42 (12) (2015) 1317–1326.
[42] A. Narayanankutty, PI3K/Akt/mTOR pathway as a therapeutic target for colorectal cancer: a Review of preclinical and clinical evidence, Curr. Drug Targets 20 (12) (2019) 1217–1226.
[43] João Machado-Neto, Fenerich Agostinho, Alves Bruna, Alves Rodrigues, Nunes Ana Paula, et al., Insulin Substrate Receptor (IRS) proteins in normal and malignant hematopoiesis, J .Clinics (Sao Paulo) 73 (2018) e566s.
[44] Rodrigues Alves Ana Paula Nunes, Fernandes Jaqueline Cristina, Fenerich Bruna Alves, et al., IGF1R/IRS1 targeting has cytotoxic activity and inhibits PI3K/AKT/mTOR and MAPK signaling in acute lymphoblastic leukemia cells, Cancer Lett. 456 (2019) 59–68.
[45] Wenli Jiang, Linghong Meng, Guangming Xu, et al., Wentilactone A induces cell apoptosis by targeting AKR1C1 gene via the IGF-1R/IRS1/PI3K/AKT/Nrf2/FLIP/Caspase-3 signaling pathway in small cell lung cancer, Oncol. Lett. 16 (2018) 6445–6457.
[46] M. Reck, J. Remon, M.D. Hellmann, First-line immunotherapy for non-small-cell lung cancer, J. Clin. Oncol.: Off. J. Am. Soci. Clin. Oncol. 40 (6) (2022) 586–597.
[47] T. Nagano, M. Tachihara, Y. Nishimura, Molecular mechanisms and targeted therapies including immunotherapy for non-small cell lung cancer, Curr. Cancer Drug Targets 19 (8) (2019) 595–630.